Journal of Molecular Structure 1199 (2020) 126997

Contents lists available at ScienceDirect

Journal of Molecular Structure

journal homepage: http://www.elsevier.com/locate/molstruc

Group 10 metal complexes with a tetradentate thiosemicarbazonate ligand: Synthesis, crystal structures and computational insights into the catalysis for C–C coupling via Mizoroki-Heck reaction

Jackelinne C. Lima [a], Rebecca D. Nascimento [b], Luana M. Vilarinho [b], Alice P. Borges [a], Leonardo H.F. Silva [c], Jhonathan R. Souza [c], Luis R. Dinelli [b], Victor M. Deflon [d], Antonio E. da Hora Machado [c, e], André L. Bogado [b], Pedro I.S. Maia [a, *]

[a] Departamento de Química, Universidade Federal do Triângulo Mineiro, Av. Dr. Randolfo Borges 1400, 38025-440, Uberaba, MG, Brazil
[b] Instituto de Ciências Exatas e Naturais do Pontal, Universidade Federal de Uberlândia, Rua vinte, 1600, 38304-402, Ituiutaba, MG, Brazil
[c] Instituto de Química, Universidade Federal de Uberlândia, Av. João Naves de Ávila 2121, 38400-902, Uberlândia, MG, Brazil
[d] Instituto de Química de São Carlos, Universidade de São Paulo, Av. Trabalhador Sãocarlense, 400, 13566-590, São Carlos, SP, Brazil
[e] Universidade Federal de Catalão, Av. Lamartine Pinto de Avelar, 1120, CEP 75704-020, Catalão, GO, Brazil

ARTICLE INFO

Article history:
Received 2 July 2019
Received in revised form
24 August 2019
Accepted 27 August 2019
Available online 28 August 2019

Keywords:
Homogenous catalysis
Thiosemicarbazones
Crystal structures
Heck catalysts
DFT

ABSTRACT

A series of mononuclear complexes has been synthesized by reactions of group 10 metal ions with bis(4-phenyl-3-thiosemicarbazone) (H_2bPht), affording compounds of general formula [M^{II}(bPht)] (M = Ni, Pd and Pt). Their characterization involved FTIR, UV–Vis, ^{1}H NMR, CV, DPV and elemental analysis. Furthermore, the crystal structures of all complexes have been determined, showing that the thiosemicarbazonate ligand is coordinated as a tetradentate *N,N,S,S*-donor forming three five-membered chelate rings. The catalytic activity of [M^{II}(bPht)] in Heck's C–C coupling reaction using styrene and iodobenzene to obtain stilbenes has been evaluated. It was verified that the Ni^{II} and Pt^{II} complexes present low catalytic activity, while the Pd^{II} complex showed a conversion of 99% within 24 h. *Trans*-stilbene was identified as the major product of the coupling reaction, up to 90%. DFT studies were also performed in order to better understand the catalytic behavior of these complexes giving support for a new route for Mizoroki-Heck reaction.

1. Introduction

Transition metal complexes derived from thiosemicarbazones (TSCs) have been widely explored in relation to their bioinorganic medicinal chemistry [1–6]. More recently, there has been an increasing interest in their catalytic applications [7–10]. Although palladium complexes have been employed successfully as catalysts in various C–C cross coupling reactions such as Negishi, Suzuki, Mizoroki-Heck and Sonogashira [11,12], the first work regarding the catalysis using a thiosemicarbazonate derived complex (Fig. 1, **I**) for Heck reaction was published only in 2004 [13]. Since then, several mononuclear Pd^{II} complexes with bidentate and tridentate TSCs (Fig. 1) have been studied as pre-catalysts for a variety of cross coupling reactions [14–22].

Most of the TSC complexes tested for such reactions are based on the mixed-ligand approach containing phosphines as the ancillary ligand (see Fig. 1, **II-V**, **VII**) [12,14–20], whose design has been probably related to the classic catalysts for C–C cross coupling reactions, such as [$Pd(PPh_3)_4$]. However, their sensitivity to oxygen requires generally inert conditions for use in catalysis [13]. Although in a lower number, homoleptic palladium complexes with TSCs have also shown to be active for cross-coupling reactions (Fig. 1, **I** and **VI**) [21,22]. Interestingly, there is only one report in the literature dealing with a bis(TSC) derivative (a dinuclear palladium(II) complex, Fig. 1, **VII**) studied as a catalyst for Mizoroki-Heck reaction [23].

Despite of the success of palladium complexes in catalysis, the high costs of palladium catalysts remain as a significant disadvantage, leading to the investigation of less expensive systems that do not decrease the efficiency. In this sense, nickel has emerged as a cheaper alternative to palladium and some Ni^{II} thiosemicarbazonate complexes have already been investigated

* Authors to whom Correspondence should be addressed.
E-mail address: pedro.maia@uftm.edu.br (P.I.S. Maia).

https://doi.org/10.1016/j.molstruc.2019.126997
0022-2860/

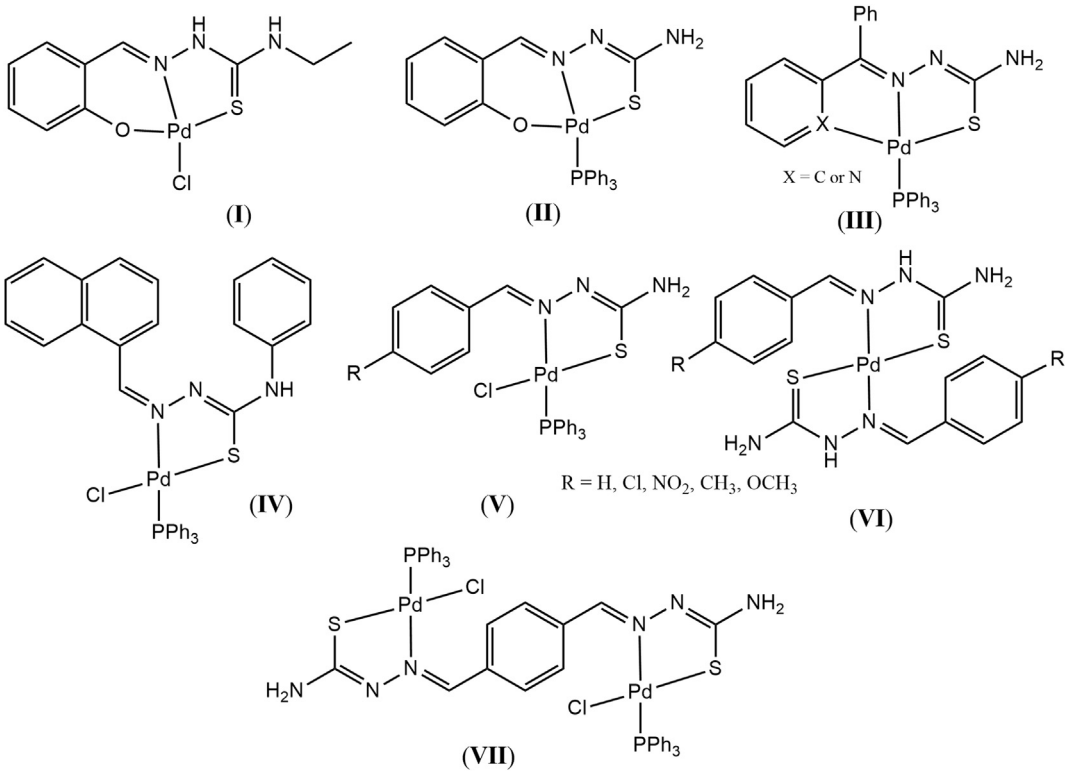

Fig. 1. Some of the Pd^{II} thiosemicarbazone catalysts for C–C coupling.

[24–27]. On the other hand, to the best of our knowledge, although many Pt^{II} complexes with TSCs have been developed for medicinal purposes, none of them have been applied as catalyst for C–C coupling until now, undoubtedly due to the expected formation of inert complexes.

Considering the context exposed above, herein we describe the synthesis and characterization of analogue Ni^{II}, Pd^{II} and Pt^{II} complexes derived from a potentially tetradentate bis(thiosemicarbazone) ligand and their evaluation as catalyst precursors for Mizoroki-Heck coupling using aryl iodide and styrene for formation of stilbenes. Based on these preliminary results, it was possible to purpose a potential catalytic pathway which was investigated by means of computational studies. To our knowledge, this paper represents the first study concerning the application of mononuclear homoleptic complexes with a bis(thiosemicarbazone) ligand in the Heck reaction.

2. Experimental

2.1. Materials and instruments

$NiCl_2 \cdot 6H_2O$ (Kinetics), 4-phenylthiosemicarbazide, 1,5-cyclooctadiene (COD) and benzil (Sigma Aldrich) and solvents were obtained from commercial sources and used without further purification. The precursors $[PtCl_2(COD)]$ and *trans*-$[PdCl_2(MeCN)_2]$ as well as the H_2bPht ligand were synthesized according to procedures described in the literature [28–30]. The melting points were determined using a PF1500 FARMA-GEHAKA instrument. The conductivities of the complexes were measured in 10^{-3} mol L^{-1} dichloromethane or dimethylsulfoxide solutions using a CG1800-GEHAKA conductometer. The elemental analyses (CHNS) were determined using a PerkinElmer CHNS/O 2400 Series II equipment. The FTIR spectra were measured on a Frontier Single Range-MIR PerkinElmer FT-IR spectrophotometer in the region between 220 and 4000 cm^{-1}. The samples were analyzed in the solid state using the Attenuated Total Reflectance (ATR) accessory with diamond crystal. The electronic spectra were measured with a Shimadzu UV-1800 spectrophotometer from DMF solutions. The ^1H NMR spectra were acquired on a Bruker Avance III HD, operating at 400 MHz. The characteristic peaks of the solvents or TMS were used as internal standards. The high resolution ESI-TOF mass spectra were obtained in a Bruker Compass micrOTOF-Q Mass Spectrometer and detected on a positive mode.

2.2. Synthetic procedures

2.2.1. Synthesis of the nickel and palladium complexes

These compounds were synthesized from equimolar reactions of H_2bPht and the desired metal precursor. Briefly, 0.2 mmol of H_2bPht (102 mg) was added to a solution containing 0.2 mmol of $NiCl_2 \cdot 6H_2O$ (64 mg) or $[PdCl_2(MeCN)_2]$ (52 mg) dissolved in EtOH (5 mL). The resulting mixtures were refluxed for 3 h and then kept under stirring for 24 h. After that, the solutions were left at −15 °C for 24 h. The precipitates formed were filtered off, washed with *n*-hexane and dried under vacuum.

Benzil bis(4-phenyl-3-thiosemicarbazonate)nickel(II) [Ni^{II}(bPht)] (**1**): Color: brown. Yield 87% (40 mg). M.P.: >300 °C. Anal. Calcd. for $C_{28}H_{22}N_6NiS_2$ (613.06 g/mol): C: 59.49; H: 3.92; N: 14.87; S: 11.34%. Found: C: 58.68; H: 4.09; N: 14.71; S: 11.27%. IR (ATR/cm^{-1}) 3298 ν(N–H), 1596 ν(C=N), 1493 ν(C=C), 720 ν(C–S). ^1H NMR (400 MHz, DMSO-d_6, δ/ppm): 10.21 (s, 2H NHPh), 7.46 (d, 4H, Ph), 7.35–7.24 (m, 10H, Ph), 7.17 (t, 4H, Ph), 6.98 (t, 2H, Ph). Molar conductivity (1×10^{-3} mol/L in CH_2Cl_2): 0.00 μS/cm. UV–Vis bands from DMF solution λ_{max}/nm (log ε): 321 (3.95), 418 (3.51), 491 (3.68).

Benzil bis(4-phenyl-3-thiosemicarbazonate)palladium(II) [Pd^{II}(bPht)] (**2**): Color: dark green. Yield 92% (112 mg). M.P.:> 300 °C.

Elemental analysis calculated for $C_{28}H_{22}N_6PdS_2$ (613.06 g/mol): C: 54.86; H: 3.62; N: 13.71; S: 10.46%. Found: C: 53.95; H: 3.63; N: 13.34; S: 10.18%. IR (ATR/cm^{-1}): 3315 ν(N–H), 1593 ν(C=N), 1446 ν(C=C), 720 ν(C–S), 1647 ν(C=N). ^{1}H NMR (400 MHz, DMSO-d_6, δ/ppm): 10.28 (s, 2H, NHPh), 7.44 (d, 4H, Ph), 7.33–7.27 (m, 10H, Ph), 7.15 (t, 4H, Ph), 6.97 (t, 2H, Ph). Molar conductivity (1×10^{-3} mol/L in CH_2Cl_2): 0.12 μS/cm. UV–Vis bands from DMF solution λ_{max}/nm (log ε): 310 (4.30), 415 (4.00), 481 (3.96).

2.2.2. Synthesis of the platinum complex

0.2 mmol of H_2bPht (102 mg) was added to a solution containing 0.2 mmol of [$PtCl_2$(COD)] (75 mg) dissolved in MeCN (5 mL). After addition of 0.5 mL of Et_3N, the resulting mixture was kept under stirring at room temperature for 24 h. The precipitate formed was filtered off, washed with *n*-hexane and dried under vacuum.

Benzil bis(4-phenyl-3-thiosemicarbazonate)platinum(II) [Pt(bPht)] (**3**): Color: green. Yield 57% (80 mg). M.P:> 300 °C. Elemental analysis calculated for $C_{28}H_{22}N_6PtS_2$ (701.73 g/mol): C: 47.92; H: 3.16; N: 11.98; S: 9.14%. Found: C: 46.83; H: 3.36; N: 11.59; S: 8.94%. IR (ATR/cm^{-1}): 3310 ν(N–H), 1588 ν(C=N), 1453 ν(C = C), 724 ν(C–S). Molar conductivity (1×10^{-3} mol/L in CH_2Cl_2) 0.06 μS/cm ^{1}H NMR (400 MHz, DMSO-d_6, δ/ppm): 10.35 (s, 2H, NHPh), 7.41 (d, 4H, Ph), 7.34–7.26 (m, 10H, Ph), 7.15 (t, 4H, Ph), 6.95 (t, 2H, Ph). UV–Vis bands from DMF solution λ_{max}/nm (log ε): 317 (3.54), 400 (3.21), 477 (3.54).

2.3. Crystal structure determinations

Good quality crystals of the complexes **1**–**3** were obtained from recrystallization from dichloromethane:ethanol (2:1) at room temperature. The data collections were performed with Mo-Kα radiation (λ = 0.71073 Å) on a BRÜKER APEX II duo diffractometer. Standard procedures were applied for data reduction and absorption correction. The structures were predicted by direct methods using SHELXS-97 [31] and refined by using SHELXL2014 [31]. The O–H bond distances for the water molecule in the crystal structure of the complex **1** were fixed using the DFIX command of SHELX2014. The positions of the other hydrogen atoms were calculated in idealized positions and treated with the "riding model" option of the SHELXL2014 program [31]. Crystallographic data and experimental details of the structural analysis are summarized in Table 1.

2.4. Electrochemical studies

The cyclic and differential pulse voltammograms were obtained from a potentiostat/galvanostat Autolab model μAutolab III coupled to a graphical interface GPES version 4.9. The measurements were carried out in a glass electrochemical cell with a capacity of 5 mL with a 3 electrode system consisting on a reference electrode (Ag/AgCl), a platinum working and counter electrodes. Tetrabutylammonium hexafluorophosphate (TBAH) at the concentration of 0.1 mol L^{-1} in CH_2Cl_2 was used as supporting electrolyte.

2.5. Gas chromatography

The catalytic yields were determined by gas chromatography using hexadecane (14.6 μL) as an internal standard. The operating conditions were optimized in an isotherm for the separation of reaction products, obtaining the following parameters: furnace temperature 170 °C, detector temperature 250 °C, injector temperature 220 °C, gas flow 2.50 mL min^{-1} constant and analysis time of 20 min. Characteristics of the NST-100 column used (Capillary column for gas chromatography, polar phase (Polyethylene Glycol - PEG), dimensions: length 30 m, internal diameter 0.25 mm, film thickness 0.25 μm). The chromatograms were also obtained in a Shimadzu model, CG-17 A coupled to a graphical interface, Shimadzu CG-Glass software version 2.0.

2.6. Theoretical calculations

The structures were optimized using the Density Functional Theory (DFT) functional M06 [32] combined with the basis set: DZP-DKH [33]. The structures, after optimization, did not present imaginary vibrational frequencies, indicating that they were structures of minimal energy. The crystallographic data were

Table 1
Refinement data for complexes [Ni(bPht)]·H_2O (**1**·H_2O), [Pd(bPht)] (**2**) and [Pt(bPht)] (**3**).

	1·H_2O	2	3
Formula	$C_{28}H_{24}N_6NiOS_2$	$C_{28}H_{22}N_6PdS_2$	$C_{28}H_{22}N_6PtS_2$
Fw	583,36	613.03	701.72
T (K)	296(2)	296(2)	296(2)
Crystal system	Monoclinic	Monoclinic	Monoclinic
Space group	$P2_1/c$	$C2/c$	$C2/c$
a (Å)	22.1848(8)	15.5945(3)	15.5929(5)
b (Å)	5.6617(2)	13.8463(3)	13.8590(4)
c (Å)	23.3488(8)	13.3872(3)	13.3162(4)
β (°)	117.816(2)	119.1070(10)	118.9930(10)
V (Å^3)	2593.82(16)	2525.59(9)	2517.03(13)
Z	4	4	4
ρ_{calcd} (g·cm^{-3})	1.494	1.612	1.852
μ (mm^{-1})	0.944	0.931	5.771
Theta range for data collection	1.038 to 25.111	2.097 to 25.091	2.095 to 26.422
Index ranges	−26←h←26, −5←k←6, −27←l←27	−16←h←18, −16←k←11, −15←l←10	−19←h←19, −17←k←17, −16←l←16
Reflections Collected	16811	7575	22549
Reflections unique/R_{int}	4602/0.0368	2214/0.0189	2588/0.1213
Data/restraints/param.	4602/2/349	2214/0/168	2588/0/169
Absorption correction	Multi-scan	Multi-scan	Multi-scan
Max/min. transmission	0.7452/0.6716	0.7452/0.6933	0.7452/0.5770
R_1 [$I > 2\sigma(I)$]	0.0390	0.0220	0.0226
wR_2 [$I > 2\sigma(I)$]	0.1108	0.0505	0.0542
GOF on F^2, *S*	1.082	1.041	1.048
Extinction coefficient	Not refined	Not refined	0.00507(17)

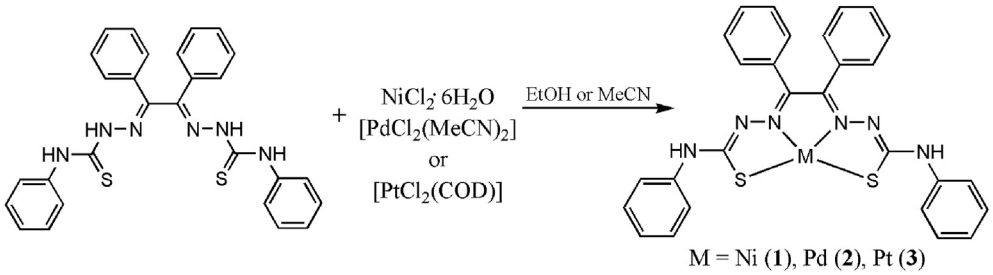

Scheme 1. Synthesis of the complexes.

compared to the optimized structures. All calculations were performed considering the isolated molecules, using the software Gaussian 09 revision E.01 [34]. The molecular orbitals, Mulliken charges and structures were represented with the aid of the software GaussView 5.0.8 [35]. In addition, the calculations related to the transition states and intermediates were executed using the DGDZVP atomic basis set and model IEFPCM [36], considering *N,N*-dimethylformamide as solvent at 393.15 K [37].

3. Results and discussion

3.1. Synthesis and spectroscopic characterization

The complexes derived from benzyl bis(4-phenyl-3-thiosemicarbazone) (H_2bPht) were obtained by reaction with the precursors $NiCl_2·6H_2O$, $[PdCl_2(MeCN)_2]$ or $[PtCl_2(COD)]$ according to Scheme 1. The Pd^{II} and Pt^{II} products present low solubility in DMSO, $CHCl_3$ and CH_2Cl_2, and are insoluble in MeCN, MeOH or EtOH, while the Ni^{II} complex is soluble in all these solvents. The molar conductivity for 10^{-3} mol L^{-1} solutions of the complexes **1**–**3** in dichloromethane presented values close to 0 μS cm^{-1}, which corresponds to the neutral form of the compounds. The elemental analyses were consistent with the general formula [M(bPht)].

Table 2
Selected bond lengths (Å) and angles (°) for the complexes [Ni(bPht)]·H_2O (**1**·H_2O), [Pd(bPht)] (**2**) and [Pt(bPht)] (**3**).

Bond lengths (Å)	(1·H_2O)	(2)	(3)
M-N(1)/N(1′)	1.856(2)/1.839(2)	1.9757(17)	1.974(2)
M-S(1)/S(1′)	2.1324(9)/2.1513(9)	2.2957(6)	2.2907(7)
C(1)–S(1)/C(1′)-S(1′)	1.753(3)/1.769(3)	1.772(2)	1.771(3)
C(2)–N(1)/C(2′)-N(1′)	1.313(4)/1.312(4)	1.310(3)	1.315(4)
C(1)–N(2)/C(1′)-N(2′)	1.317(4)/1.301(4)	1.309(3)	1.309(4)
Bond Angles (°)			
N(1)-M-N(1′)	83.69(11)	80.72(10)	80.46(13)
N(1)-M-S(1′)/N(1′)-M-S(1)	171.29(8)/171.49(8)	164.71(5)	164.60(7)
N(1)-M-S(1)/N(1′)-M-S(1′)	87.85(8)/87.73(8)	84.36(5)	84.44(7)
C(1)-S(1)-M/C(1′)-S(1′)-M	94.56(10)/93.98(10)	93.51(7)	93.48(10)
N(2)-N(1)-M/N(2′)-N(1′)-M	123.51(19)/124.01(19)	123.75(14)	123.81(18)
S(1)-M-S(1′)	100.71(4)	110.71(3)	110.79(4)

The infrared spectra of the analogous complexes [M^{II}(bPht)] show only small differences. The spectrum of the free ligand shows two bands at 3337 and 3260 cm^{-1} for the $\nu_{(NH)}$ stretch, while in the spectra of complexes **1**–**3** (see SI) only one absorption was found, at 3298, 3315 and 3310 cm^{-1}, respectively. This fact is expected due to deprotonation of the ligand upon coordination. The vibrations attributed to the $\nu_{(C{=}N)}$ stretches, found at 1599 cm^{-1} for H_2bPht, undergo small shifts upon formation of the complexes **1**, **2** and **3**, being observed respectively at 1596, 1593 and 1588 cm^{-1}. The $\nu_{(C{=}S)}$ band, observed at 874 cm^{-1} for H_2bPht, is also shifted to smaller wavenumbers after coordination, which is in agreement with the formation of the C–S bond after coordination, corroborating with *NNSS*-coordination mode of the ligand [3–5].

The ^{1}H NMR spectrum of the free ligand (Fig. S5) shows two signals related to the NH groups, at 10.43 and 10.48 ppm, while the spectra of the complexes **1**–**3** (Figs. S6–8) present only one signal in the range 10.2–10.4 ppm, according to the deprotonation of the ligand as indicated by the IR data. The signals related to the phenyl rings, found in the range 7.21–7.86 ppm for the free ligand, suffer a shielding effect upon complexation which is dependent on the metal center. Due to the low solubility, the characterization by ^{13}C NMR was not possible.

3.2. Crystal structures

The crystal structures of the complexes **1**, **2** and **3** were determined by single crystal X-ray diffraction. Selected bond lengths and angles are shown in Table 2. Figs. 2 and 3 show the molecular structures of the complexes [Ni(bPht)] and [Pd(bPht)] as

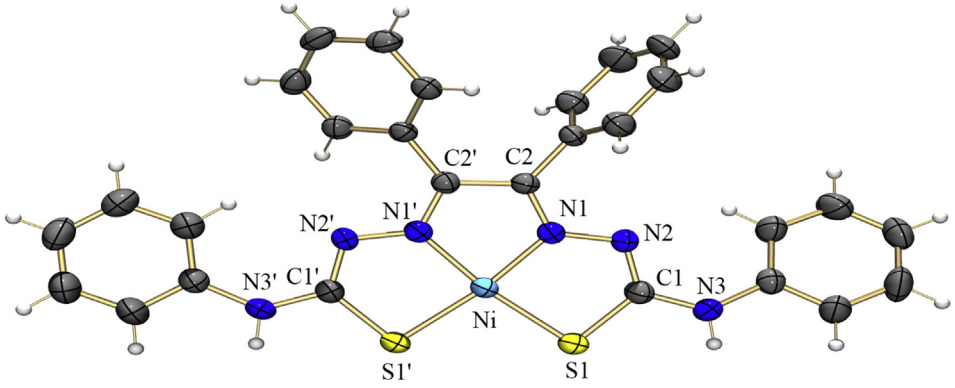

Fig. 2. ORTEP representation of the complex [Ni(bPht)] (**1**) with thermal ellipsoids at 50% probability. Water molecule has been omitted for clarity.

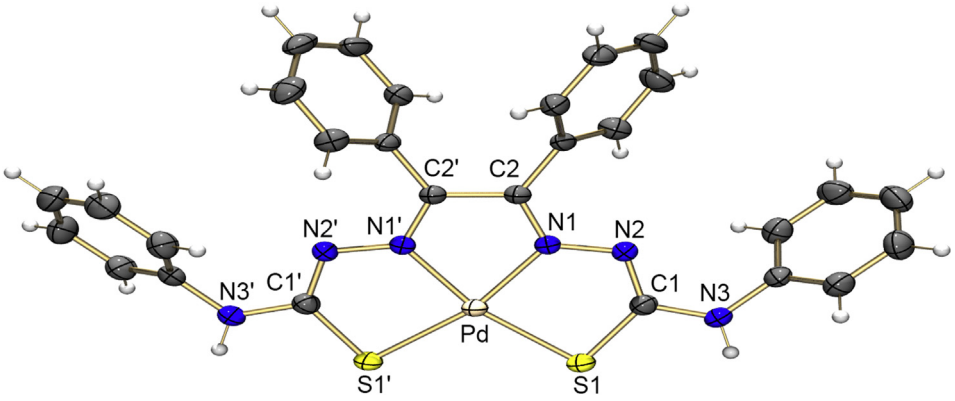

Fig. 3. ORTEP representation of the complex [Pd(bPht)] (**2**) with thermal ellipsoids at 50% probability. Symmetry operation used to generate equivalent atoms ('): x+3, -y+1, -z+1.

representative of these compounds. [Pd(bPht)] is isostructural with the platinum derivative and crystallizes in the monoclinic system and space group *C2/c*, while [Ni(bPht)] crystallizes in the monoclinic and space group $P2_1/c$. An ORTEP representation of the complex **3** can be observed in the SI (Fig. S9). For the complexes **2** and **3** only half molecule is observed in the asymmetric unit. Another crystal structure for the Pt^{II} derivative containing acetone as solvate in triclinic system and space $P\bar{1}$ has already been published by our group [38].

The coordination geometry around the Ni^{II}, Pd^{II} and Pt^{II} metal centers is best described as a distorted square-planar with high distortions at the N(21)-M-S(11) angle (171.49(8), 164.71(5) and 166.5(9) ° for M = Ni, Pd and Pt, respectively). In all the complexes the thiosemicarbazone ligand coordinates to the metal center as a *NNSS*-donor with double deprotonation of the coordinating backbone, forming three five-membered chelate rings, with metal ions lying in an approximate plane with the four donor atoms (deviations: 0.0179, 0.0167 and 0.0157 Å, for M = Ni, Pd and Pt, respectively). The Ni—S and Ni—N bond lengths are significantly shorter than those for the Pd and Pt complexes which is consistent with the smaller ionic radius of Ni^{II}. This fact also reflects on the considerable differences among the angles involving the metal centers. The C—S bond length, of 1.6764(18) Å for H_2bPht [28], suffers an increase to 1.769(32) Å, 1.772(2) and 1.85(4) Å upon formation of the complexes **1**, **2** and **3**, respectively, which can be explained by the deprotonation of the nitrogen atoms N2/N2' and consequent coordination in the thioenolate form of the ligand. This is also in accord with the decrease carbon-hydrazinic nitrogen bond distance from 1.372(2) Å in the free ligand to approximately 1.31 Å in the complexes.

The crystal structure of the complex **1** contains a co-crystallized water molecule. The water molecule forms an intermolecular hydrogen bond network involving the oxygen atom O1s as H-donor and receptor to the sulfur atoms S2′ and nitrogen atom N3', respectively (see Fig. 4). The second NH group also works as a hydrogen donor to the sulfur atom S1b from a symmetry related molecule. In the crystalline net of the complexes **2** and **3** no water molecule was observed and also no H-bond.

3.3. Electrochemical studies

The redox potential of a complex is determinant for its catalytic activity. By the redox potential, it is possible to verify the stability of the complexes against oxidation or reduction, since complexes with higher redox potential will be more stable with respect to the formation of species with higher oxidation states. In addition, there

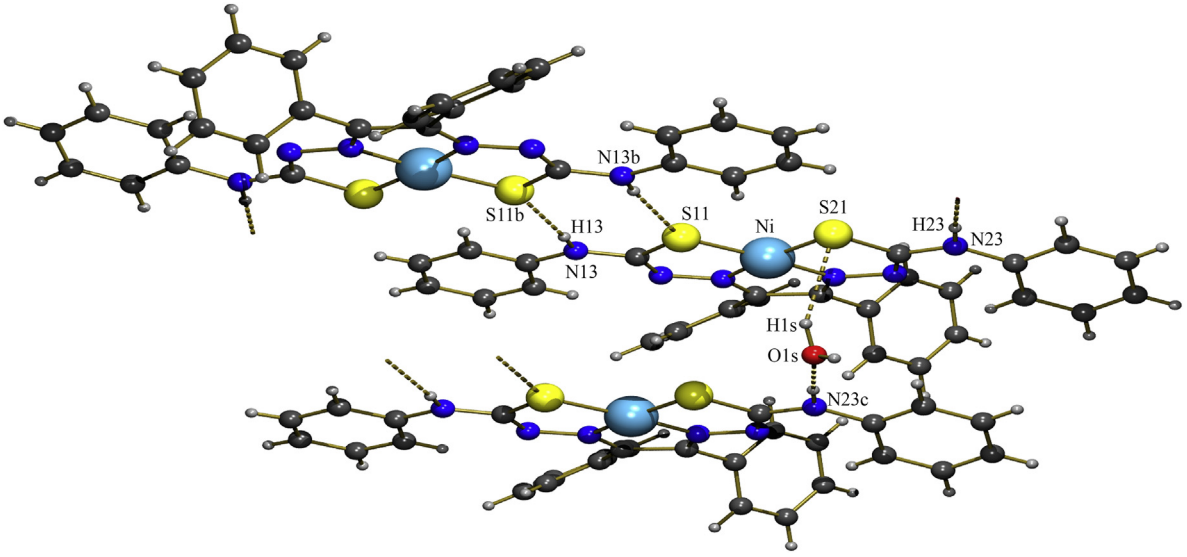

Fig. 4. Hydrogen bonds found in the crystalline structure of [Ni(bPht)]•H_2O. [N(3′) … O(1S′) = 2.919(5) Å, N(23)—H(23) … O(1S′) = 173.6°], [N(3) … S(1b) = 3.467(3) Å, N(3)—H(3) … S(1b) = 172.5°] and [O(1S)···S(1′) = 3.529(5) Å, O(1S)— H(1S)···S(1′) = 142(4) °]. Symmetry operations: (b) x, y+1, z and (c) -x+1, -y+2, -z+1.

Table 3
Electrochemical data of complexes **1**, **2** and **3** (Ag/AgCl, 0.1 mol L^{-1} HTBA solution in CH_2Cl_2, 50 mV/s).

Complex	E_{ap} (V)	E_{cp} (V)	ΔE_p[a] (mV)	$E_{1/2}$[b] (V)
1	0.99	1.03	40	1.01
	1.27	1.31	40	1.29
2	1.07	1.13	60	1.10
	1.37	1.43	60	1.40
3	0.95	1.04	90	1.00
	1.39	1.43	40	1.41

[a] $\Delta E_p = E_{ap} - E_{cp}$.
[b] $E_{1/2} = (E_{ap} + E_{cp})/2$.

are few reports in the literature involving electrochemical studies with complexes of group 10 metals and thiosemicarbazones. In order to understand the redox behavior of the compounds presented in this work, cyclic voltammetry experiments for the free ligand and its complexes **1**–**3** were carried out in CH_2Cl_2 solution using tetrabutylammonium hexafluorophosphate (TBAH) as supporting electrolyte.

No redox potential was verified for the free ligand within the analyzed range (Fig. S10). Table 3 shows the data obtained for the complexes. Fig. 5 presents the voltammograms of the complexes **1** and **2** as representative for the complexes. In the cyclic voltammogram of the complex [Ni(bPht)] (**1**) two anodic (Ni^{II}/Ni^{III} and Ni^{III}/Ni^{IV}) and two cathodic (Ni^{IV}/Ni^{III} and Ni^{III}/Ni^{II}) processes have been clearly observed, characterizing two reversible processes (I_{pa}/I_{pc} ratio ≈ 1 and $\Delta E_p < 59$ mV) [39]. This electrochemical behavior is similar to that observed for other nickel complexes derived from thiosemicarbazones [40], however, it can be modified according to the substituents of the ligand [41]. In the CV of the complexes **2** and **3** (see Fig. S11), apparently, only one clear anodic process was recorded at approximately 1.11 and 1.03 V, respectively. However, looking more deeply into the CV of these complexes it is possible to observe also discrete cathodic potentials. In order to confirm this remark, the differential pulse voltammetry analysis, a more sensitive technique, was used, showing two cathodic and two anodic processes with large intensity, as verified for the nickel derivative (Fig. 5 and Fig. S12). Thus, it was verified that all the complexes studied here present two reversible or quasi-reversible processes supposed to be related to the M^{II}/M^{III} and M^{III}/M^{IV} redox couples. Only one reference describing the electrochemical behavior of palladium complexes with thiosemicarbazones was found in the literature, but the complexes have a different behavior, presenting one redox process at positive potentials, attributed to the Pd^{II}/Pd^{III} pair, and a second one at negative potentials, which was ascribed as Pd^{II}/Pd^{I} [42]. It was also verified that the metal centers influence the redox potentials and that palladium complex (**2**) showed the highest oxidation potential for the first process ($E_{1/2} = 1.10$ V) and higher than that of the nickel complex (**1**) for the second process ($E_{1/2} = 1.40$ V). Overall, the high oxidation potentials (close to 1 V) found for the complexes here show that the electron withdrawing groups of the ligand lead to a high stability of the oxidation state of the metal centers.

3.4. Catalytic efficiency in Mizoroki-Heck reaction

Our methodology employed Ni^{II}, Pd^{II} and Pt^{II} complexes as pre-catalysts as described in Scheme 2, there is the possibility of formation of three products, however, the diphenylethene was not observed by gas chromatography**.** The reactions of iodobenzene with styrene were studied by varying the amount of pre-catalyst in order to verify a possible catalytic activity of the complexes.

Tests for coupling reactions of the Heck type, performed to obtain products with the structure of stilbenes, indicated that complexes derived from bis(thiosemicarbazones) exhibit catalytic

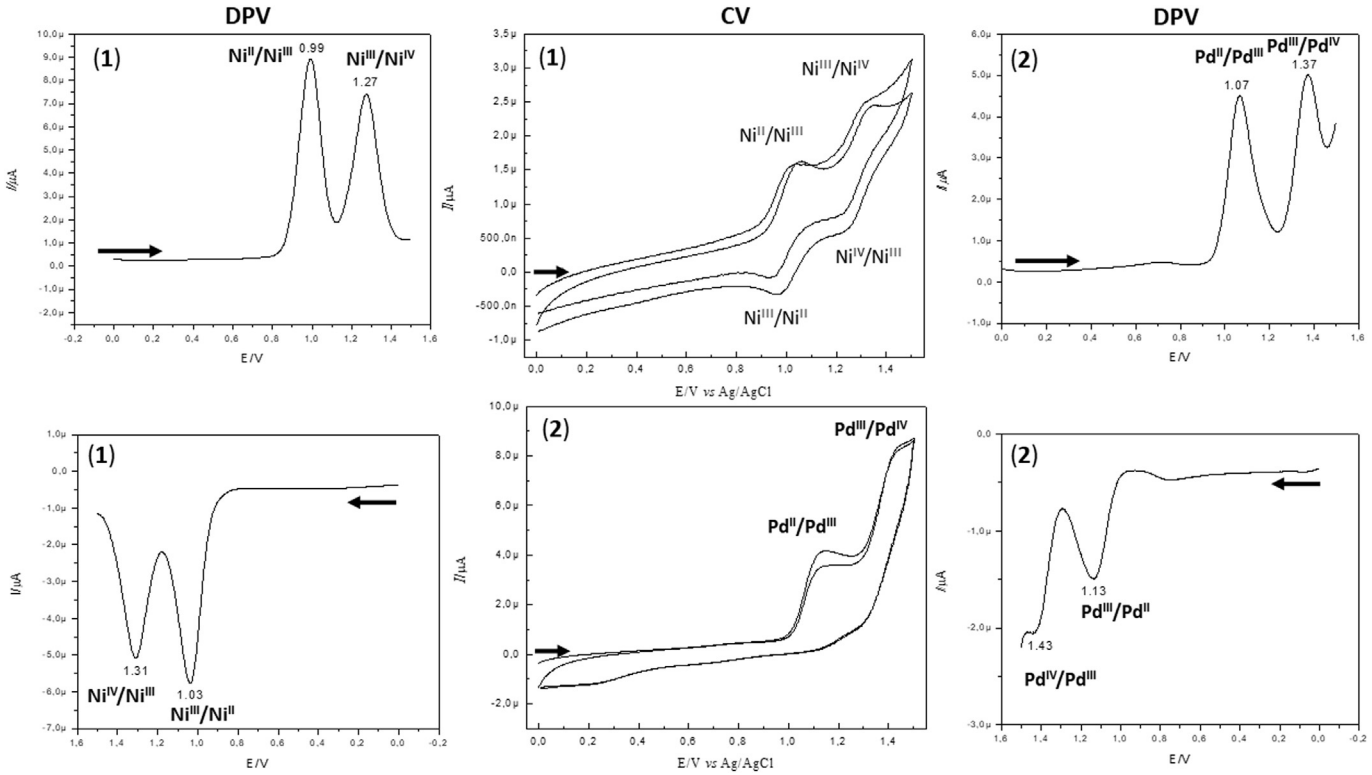

Fig. 5. Differential pulse voltammograms (DPV) and cyclic voltammograms (CV) of the complexes **1** and **2** (Ag/AgCl, 0.1 mol L^{-1} HTBA solution in CH_2Cl_2, 50 mV/s).

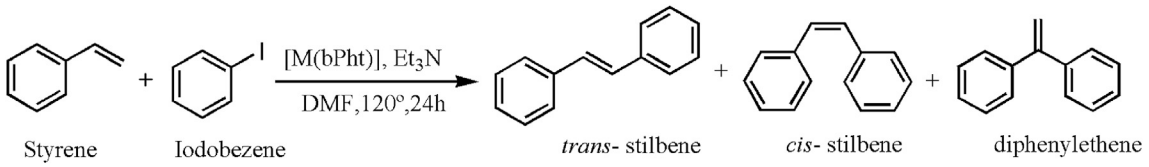

Scheme 2. Heck reaction between styrene and iodobenzene catalyzed by [M^{II}(bPht)] (M = Ni, Pd or Pt).

activity. The achieved conversions are shown in Table 4.

It was possible to observe that the palladium pre-catalyst has a good activity in DMF as solvent, at 3.5 mol %, within 12 h of reaction. The analysis of the aliquot indicates 85% of conversion to products when the Pd pre-catalyst was used, while in the presence of Ni and Pt pre-catalysts no reaction was observed at the same time. When the reaction was carried out in a period of 24 h, under the same conditions, a conversion of 99% was verified for the Pd pre-catalyst. The Ni and Pt catalysts were also active with 24 h of reaction, but presented lower conversion rates when compared to the Pd system.

Since the Pd pre-catalyst presented interesting results, further studies were performed. The first experiment was to attest the influence of the concentration of pre-catalyst in the reaction. Hence, the amount of the Pd pre-catalyst was doubled (7 mol %) and reduced to (1.75 mol %). When in a higher concentration, it was possible to verify the formation of 99% of the products after 12 h of reaction. However, no catalytic activity was detected upon reduction of the amount of catalyst to 1.75%. Standard catalysts of palladium such as [$Pd(PPh_3)_4$] and [$Pd(OAC)_2$] have a conversion rate in the range of 50–92% at 120 °C [43], while a variation from 11% to 99% has been reported for non-standard palladium complexes [44–47], which shows that the palladium catalyst used this work is very promising.

The catalytic activity of the palladium complex was also carried out *in situ* reaction, using 3.5 mol % of Pd-precursor and the free thiosemicarbazone ligand within 12 h of reaction, at reflux in DMF solution, but no conversion to products was found. Nevertheless, when the time was increased to 24 h, a conversion of 60% was found. This fact indicates that the catalyst can be generated *in situ*, although a long time of induction is required to produce the real catalyst.

The products of the reaction catalyzed by Pd^{II} were analyzed by ^{1}H NMR (see Fig. S13). Hydrogen signals from ethene were observed as a singlet peak at 7.10 ppm. A doublet at 7.50 ppm and two triplet signals at 7.35 and 7.25 ppm correspond to the aromatic hydrogen atoms. Signals at 1.26 and 0.86 ppm are due to the presence of *n*-hexane used in product separation.

In addition to the ^{1}H NMR analysis, the product formed in the palladium reaction was also characterized by gas chromatography (Fig. S14), being possible to observe two signals at the times of 10.35 and 21.45 min. For the identification of these products, commercial *cis*-stilbene and *trans*-stilbene were used as standards, which had retention times of 10.35 and 21.45 min, respectively (see Table S1). Therefore, it is possible to state that the products obtained from the catalyzed reactions were *cis*-stilbene and *trans*-stilbene.

A new test was carried out to verify the influence of the time on the C–C coupling reaction. The aliquots were withdrawn at 0, 1, 3, 5, 7, 9 and 24 h. From the calculations performed it was possible to determine the conversion rate, yield and selectivity of the Pd^{II} pre-catalyst in the Heck reaction of styrene and iodobenzene. These data are presented in Table 5. Surprisingly, after the catalytic reaction, the solution which was left under slow evaporation afforded green crystals. These crystals were not suitable for X-ray diffraction, however, by mass spectrometry analysis (Fig. S15) it was possible to suggest that the Pd-complex seems to be regenerated since the ESI^+ HRMS spectrum shows the molecular ion peak $[M + H]^+$ with the expected isotopic pattern of the initial complex **2** (*m/z* (100% of relative isotopic abundance) found/calculated = 613.0456/613.0460) (see Fig. S16). Another peak found at *m/z* = 1227.0760 is in accord with an adduct of $[2\ M + H]^+$ (*m/z* (calcd) = 1227.08467) (see Fig. S17).

3.5. DFT studies

3.5.1. Optimized structures and orbitals of the complexes

In order to better understand the catalytic activity of the complexes, DFT calculations were performed. The optimized structures can be observed in Figs. S18–20 (Supplementary Information), presenting a high similarity among them. Selected theoretical bond lengths and angles along with a comparison with experimental values are shown together in Table S2. The calculated values for the geometric parameters suggest good agreement with the structures elucidated by X-ray crystallography, as shown by the calculated deviations, demonstrating that the calculated structures are very similar to the crystalline ones. The highest discrepancies were observed for the Pt^{II} complex, in the immediate coordination environment around the platinum center, with some overestimation of the angle between the metal and the adjacent nitrogen atoms (N(1)-Pt-N(1′), 11.4%), and between the neighboring nitrogen atoms and the metal (N(2)-N(1)-Pt, 7.10%). An inference

Table 4
Heck reactions of iodobenzene and styrene in DMF (120 °C) at 12 h and 24 h.

Complex	Mol%	Conversion (%) at 12 h	Conversion (%) at 24 h
1	3.5	0	19
2	3.5	85	99
3	3.5	0	22
2	1.75	0	0
2	7	99	99
2 (*in situ*)	3.5	0	60

Reactions were carried out in DMF (3.0 mL), in the presence of iodobenzene (60 μ L, 0.54 mmol), styrene (90 μ L, 0.79 mmol), NEt3 (96 μL, 0.69 mmol) and pre-catalyst (19 μ mol) at 120 °C. [M]/iodobenzene/styrene/NEt3 molar ratio = 1/28/42/36. a Conversion of products were determinate by gas chromatography using *n*-hexadecane as internal standard.

Table 5
Heck reactions of iodobenzene and styrene using [Pd(bPht)] (3.5 mol%) as the catalyst at different times using DMF (120 °C) as solvent.

Time (h)	Conversion[a]	Selectivity *cis/trans* (%)[b]	
		cis-stilbene (%)	*trans*-stilbene (%)
0	–	–	–
1	–	–	–
3	–	–	–
5	67.30	11.91	88.10
7	77.52	10.07	89.92
9	74.55	12.85	87.15
24	81.66	12.30	87.70

[a] GC conversion determined by internal standard (IS = *n*-hexadecane).
[b] Selectivity = yield of product/conversion × 100.

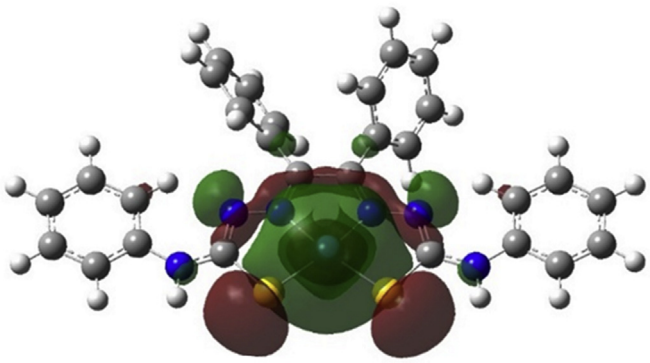

Fig. 6. HOMO orbital for the complex [Pt(bPht)] (**3**).

made involving a distinct set of atomic bases (result not shown) suggests that the observed discrepancy may be related to the inherent characteristics of the set of bases used which, however, does not compromise the quality of the results.

The HOMO relative to the three complexes studied are represented below (Figs. 6 and 7). It can be observed that the electron distribution in the frontier state of the Pt^{II} complex differs significantly from that observed for the others, most probably due to the participation of electrons in the 4f sublevel of the metal center (see Fig. 6), which indicates that in catalytic terms the Ni^{II} and Pd^{II} complexes should have similar trends (see Fig. 7), but differing from the Pt^{II} one. Considering the Pd^{II} and Ni^{II} complexes, there is a clear inversion in the polarity of the wave functions between them as well as the existence of a d_{xz} orbital on the metal center (which presents a higher density for Pd^{II}).

Besides, the analysis of Mulliken's partial atomic charges on the metal ions and neighboring ligands (see Table S3 and Figs. S21–23) shows positive charges on Ni^{II} (+0.284) and Pd^{II} (+1.154), being the charge on Pd^{II} four times. On the other hand, the value for Pt^{II} is comparable to that of Ni^{II}, but with a negative signal (−0.273), which could provide the different behavior for the Pt^{II} complex. This fact is in accord with the first oxidation potentials of the complexes **1** (0.99 V), **2** (1.07 V) and **3** (0.95 V). Besides, the fact that the partial charge on Pd^{II} is about four times higher than that on Ni^{II}, together with the higher efficiency of the Pd^{II} complex in the catalytic process, indicates that the first step of the catalysis is possibly an oxidative addition of iodobenzene via an ionic pathway [48].

3.5.2. Calculated reaction pathway

The first step in the mechanism proposal involves an oxidative addition in the Pd-complex from iodobenzene to provide a Pd^{IV} intermediate (Fig. 8). The variation of Gibbs free energy (ΔG°_{r}) in this step was determined as − 3.18 k*J* mol^{-1}. The second step consists of a nucleophilic attack from styrene and a consecutive aryl migratory 1,2-insertion, providing an 18-electron σ-intermediate. This last step has a remarkable $\Delta G^{\circ}_{r} = -265 \times 10^{6} J\ mol^{-1}$. The third step encompasses the formation of a pre-product by a reductive elimination assisted by a β-elimination by iodine attack to produce the initial Pd^{II} complex. This step showed a $\Delta G^{\circ}_{r} = -1329$ k*J* mol^{-1}. Finally, the pre-product can react with NEt_3 or with I^- to provide the desired product and the respective conjugated acid. These steps were labeled as 4.1 and 4.2 (Fig. 8) and showed $\Delta G^{\circ}_{r} = -139$ k*J* mol^{-1} and −67 k*J* mol^{-1}, respectively. All steps showed a reversible work that may be performed to provide a spontaneous Heck reaction of the iodobenzene and styrene catalyzed by [Pd^{II}(bPht)]. However, attempts of reaction without addition of base have not succeeded, so the 4.1 step seems to be the most plausible. It is important to highlight that the latter conclusion is also supported by a comprehensive review of a large number of studies that reported the formation of Pd^{IV} intermediates during C–C coupling reactions [49–55].

Additionally, we have also been investigating another proposal involving a classic hydride β-elimination from the 18-electron σ-intermediate, producing a [Pd(H)(I)(bPht)] intermediate (see Table S4 in the SI), following by a reductive elimination assisted by base to produce the initial Pd^{II}-complex, the product and [$HNEt_3I$]. Nevertheless, the energy variation related to this pathway has not shown to be accessible. For while, it was only investigated by DFT calculations, but some experiments have been planned in order to confirm them, including a kinetic study.

4. Conclusions

The benzil bis(4-phenyl-3-thiosemicarbazone) ligand successfully provided analogous complexes with Ni^{II}, Pd^{II} and Pt^{II} metal centers. All compounds were suitably characterized. It was possible to verify a catalytic activity in Heck C–C coupling reactions at 24 h for all the complexes. The palladium complex showed promising results affording an excellent conversion and selectivity. The major product formed in the Heck reaction using the palladium complex was characterized as *trans*-stilbene. Interestingly, the original palladium complex could be partially recovered after use in the catalytic reaction indicating that this catalyst is regenerated. Besides, by means of DFT calculations it was possible to verify that the catalytic behavior of the complexes can be emphasized by an analysis of the frontier orbitals in each complex as well as from the Mulliken's partial atomic charges on the metal centers. The accessibility of Pd^{IV} intermediates was computationally indicated. This implies that tetradentate thiosemicarbazonate complexes

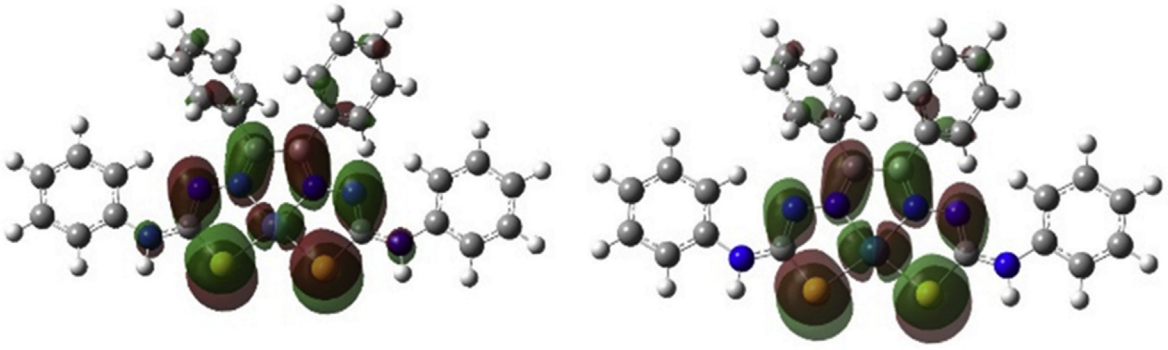

Fig. 7. HOMO orbital for the complexes [Ni(bPht)] (**1**, left) and [Pd(bPht)] (**2**, right).

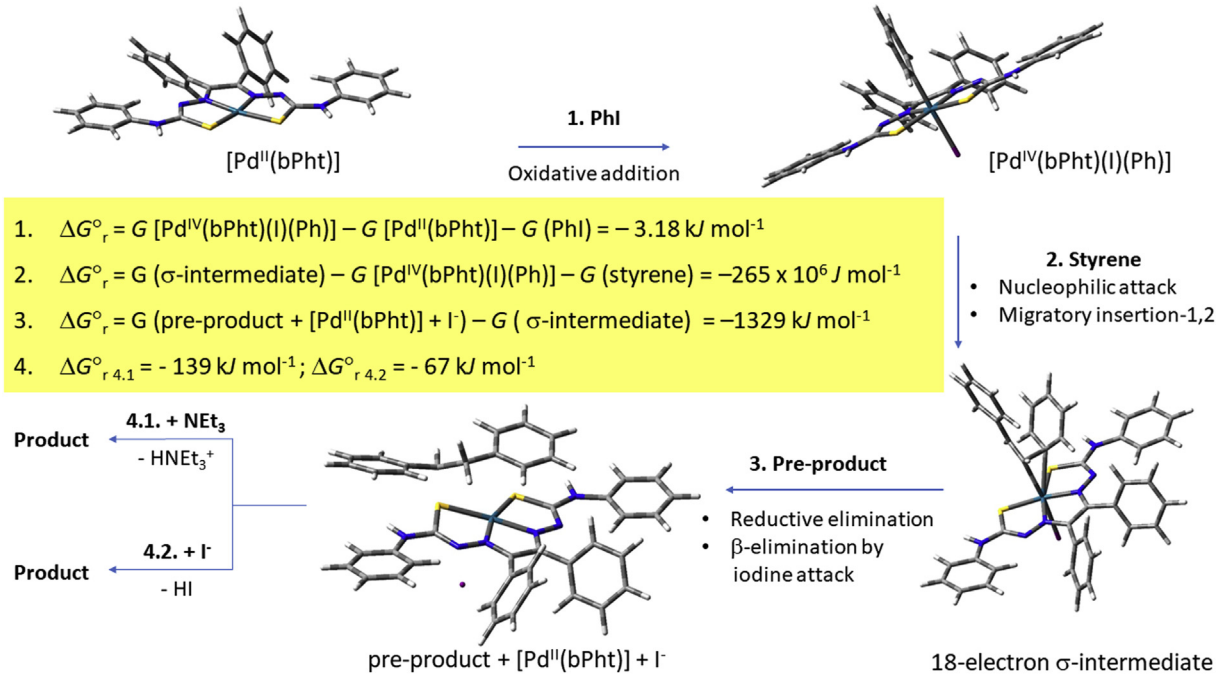

Fig. 8. Proposal of the potential mechanism of the reaction between styrene and iodobenzene catalyzed by [Pd^{II}(bPht)] (**2**), including $\Delta G°_r$ values for each step.

described here do not follow the typical reaction mechanism for Heck catalysts. Further studies using other bases as well as the investigation of experimental evidences to support the catalytic reaction pathway proposed in the present work are now ongoing.

Acknowledgements

This work was supported by CNPq (Grants 305432/2017-6, 424095/2018-1 and 307443/2015-9), CAPES, FAPESP (Grant 2009/54011-8) and FAPEMIG (Grants APQ-03174-18, APQ-01988-14, APQ-00583-13 and APQ-03017-16). This work is also a collaboration research project of members of the Rede Mineira de Química (RQ-MG) supported by FAPEMIG (Project: CEX-RED-00010-14) and of the Grupo de Materiais Inorgânicos do Triângulo-GMIT research group supported by FAPEMIG (Project: APQ-00330-14).

Appendix A. Supplementary data

Supplementary data to this article can be found online at https://doi.org/10.1016/j.molstruc.2019.126997.

References

[1] P.I.S. Maia, V.M. Deflon, U. Abram, Future Med. Chem. 6 (13) (2014) 1515–1536.
[2] M. Christlieb, J.R. Dilworth, Chem. Eur J. 12 (2006) 6194–6206.
[3] A.C.R. Gonçalves, Z.A. Carneiro, C.G. Oliveira, A. Danuello, W. Guerra, R.J. Oliveira, F.B. Ferreira, L.L.W. Veloso-Silva, F.A.H. Batista, J.C. Borges, S. de Albuquerque, V.M. Deflon, P.I.S. Maia, Eur. J. Med. Chem. 141 (2017) 615–631.
[4] P.I.S. Maia, Z.A. Carneiro, C.D. Lopes, C.G. Oliveira, J.S. Silva, S. de Albuquerque, A. Hagenbach, R. Gust, V.M. Deflon, U. Abram, Dalton Trans. 46 (2017) 2559–2571.
[5] C.G. Oliveira, P.I.S. Maia, P.C. Souza, F.R. Pavan, C.Q.F. Leite, R.B. Viana, A.A. Batista, O.R. Nascimento, V.M. Deflon, J. Inorg. Biochem. 132 (2014) 21–29.
[6] Z.A. Carneiro, J.C. Lima, C.D. Lopes, A.P.S. Gaspari, S. de Albuquerque, L.R. Dinelli, L.L.W. Veloso-Silva, M.O. Paganelli, S.H. Libardi, C.G. Oliveira, V.M. Deflon, R.J. Oliveira, J.C. Borges, P.I.S. Maia, Eur. J. Med. Chem. 180 (2019) 213–223.
[7] W. Boussebbat, A. Ounissi, Y. Farina, N. Ouddai, J. Mol. Struct. 1154 (2019) 19–26.
[8] A. Ratnam, M. Bala, R. Kumar, U.P. Singh, K. Ghosh, J. Organomet. Chem. 856 (2018) 41–49.
[9] R. Ramachandran, G. Prakash, P. Viswanathamurthi, J.G. Malecki, Inorg. Chim. Acta 477 (2018) 122–129.
[10] S. Basua, R. Acharyya, F. Basuli, S.-M. Peng, G.-H. Lee, G. Mostafa, S. Bhattacharya, Inorg. Chim. Acta 363 (12) (2010) 2848–2856.
[11] I.P. Beletskaya, F. Alonso, V. Tyurin, Coord. Chem. Rev. 385 (2019) 137–173.
[12] C.C.C.J. Seechurn, M.O. Kitching, T.J. Colacot, V. Snieckus, Angew. Chem. Int. Ed. 51 (2012) 5062–5085.
[13] D. Kovala-Demertzi, P.N. Yadav, M.A. Demertzis, J.P. Jasiski, F.J. Andreadaki, I.D. Kostas, Tetrahedron Lett. 45 (2004) 2923–2926.
[14] P. Paul, S. Datta, S. Halder, R. Acharyya, F. Basuli, R.J. Butcher, S.-M. Peng, G.-H. Lee, A. Castineiras, M.G.B. Drew, S. Bhattacharya, J. Mol. Catal. A 344 (2011) 62–73.
[15] R.N. Prabhu, R. Ramesh, Tetrahedron Lett. 58 (2017) 405–409.
[16] L. Lu, P. Chellan, G.S. Smith, X. Zhang, H. Yan, J. Mao, Tetrahedron 70 (2014) 5980–5985.
[17] P. Paul, P. Sengupta, S. Bhattacharya, J. Organomet. Chem. 724 (2013) 281–288.
[18] P. Paul, R.J. Butcher, S. Bhattacharya, Inorg. Chim. Acta 425 (2015) 67–75.
[19] J. Dutta, S. Bhattacharya, RSC Adv. 3 (2013) 10707–10721.
[20] D. Pandiarajan, R. Ramesh, Y. Liu, R. Suresh, Inorg. Chem. Commun. 33 (2013) 33–37.
[21] I.D. Kostas, G.A. Heropoulos, D. Kovala-Demertzi, P.N. Yadav, J.P. Jasinski, M.A. Demertzis, F.J. Andreadaki, G. Vo-Thanh, A. Petit, A. Loupy, Tetrahedron Lett. 47 (2006) 4403–4407.
[22] I.D. Kostas, F.J. Andreadaki, D. Kovala-Demertzi, C. Prentjas, M.A. Demertzis, Tetrahedron Lett. 46 (2005) 1967–1970.
[23] R.N. Prabhu, R. Ramesh, Tetrahedron Lett. 53 (2012) 5961–5965.
[24] Ş. Güveli, S.A. Çınar, Ö. Karahan, V. Aviyente, B. Ülküseven, Eur. J. Inorg. Chem. (2016) 538–544.
[25] R.N. Prabhu, R. Ramesh, Tetrahedron Lett. 57 (2016) 4893–4897.
[26] R.N. Prabhu, J. Lakshmipraba, Transit. Met. Chem. 42 (2017) 579–585.
[27] P.K. Suganthy, R.N. Prabhu, V.S. Sridevi, Tetrahedron Lett. 54 (2013) 5695–5698.
[28] L. Alsop, A.R. Cowley, J.R. Dilworth, P.S. Donnelly, J.M. Peach, J.T. Rider, Inorg. Chim. Acta 358 (2005) 2770–2780.
[29] J.C. Bailar, H. Itatani, Inorg. Chem. 4 (1965) 1618–1620.
[30] M.A. Andrews, T.C.T. Chang, C.-W.F. Cheng, T.J. Emge, K.P. Kelly, T.F. Koetzle, J. Am. Chem. Soc. 106 (1984) 5913–5920.
[31] G.M. Sheldrick, SHELXS-97 and SHELXL2014, Programs for the Solution and Refinement of Crystal Structures, University of Göttingen, Göttingen, Germany, 1997, 2014.
[32] Y. Zhao, D.G. Truhlar, Chem. Phys. Lett. 502 (2011) 1–13.
[33] A.C. Neto, F.E. Jorge, Chem. Phys. Lett. 582 (2013) 158–162.
[34] M.J. Frisch, G.W. Trucks, H.B. Schlegel, G.E. Scuseria, M.A. Robb, J.R. Cheeseman, G. Scalmani, V. Barone, B. Mennucci, G.A. Petersson, H. Nakatsuji, M. Caricato, X. Li, H.P. Hratchian, A.F. Izmaylov, J. Bloino,

G. Zheng, J.L. Sonnenberg, M. Hada, M. Ehara, K. Toyota, R. Fukuda, J. Hasegawa, M. Ishida, T. Nakajima, Y. Honda, O. Kitao, H. Nakai, T. Vreven, J.A. Montgomery Jr., J.E. Peralta, F. Ogliaro, M. Bearpark, J.J. Heyd, E. Brothers, K.N. Kudin, V.N. Staroverov, R. Kobayashi, J. Normand, K. Raghavachari, A. Rendell, J.C. Burant, S.S. Iyengar, J. Tomasi, M. Cossi, N. Rega, N.J. Millam, M. Klene, J.E. Knox, J.B. Cross, V. Bakken, C. Adamo, J. Jaramillo, R. Gomperts, R.E. Stratmann, O. Yazyev, A.J. Austin, R. Cammi, C. Pomelli, J.W. Ochterski, R.L. Martin, K. Morokuma, V.G. Zakrzewski, G.A. Voth, P. Salvador, J.J. Dannenberg, S. Dapprich, A.D. Daniels, Ö. Farkas, J.B. Foresman, J.V. Ortiz, J. Cioslowski, D.J. Fox, Gaussian 09, Revision E.01, Gaussian, Inc., Wallingford CT, 2015.

[35] Gaussian, Inc., Wallingford, CT, USA.

[36] N. Godbout, D.R. Salahub, J. Andzelm, E. Wimmer, Can. J. Chem. 70 (1992) 560–571.

[37] J. Tomasi, B. Mennucci, E. Cancès, J. Mol. Struct. 464 (1999) 211–226.

[38] P.I.S. Maia, F.R. Pavan, C.Q.F. Leite, U. Abram, E.S. Lang, A.A. Batista, V.M. Deflon, L. Pele, J.J. Powell, S. Kinrade, R. Jugdaohsingh, P. Collery, I. Maymard, A. Badawi (Eds.), Metal Ions in Biology and Medicine and Aqueous Chemistry and Biochemistry of Silicon, John Libbey Eurotext, Paris, 2011, pp. 164–171.

[39] P. Zanello, Inorganic Electrochemistry: Theory, Practice and Application, RSC, 2003.

[40] R. Prabhakaran, R. Sivasamy, J. Angayakanni, R. Huang, P. Kalaivani, R. Karvembu, F. Dallemer, K. Natarajan, Inorg. Chim. Acta 374 (2011) 647–653.

[41] S. Guveli, A. Koca, N. Özdemir, T. Bal-Demirci, B. Ülkiseven, New J. Chem. 38 (2014) 5582–5589.

[42] R. Prabhakaran, S.V. Renukadevi, R. Karvembu, R. Huang, J. Mautz, G. Huttner, R. Subashkumar, K. Natarajan, Eur. J. Med. Chem. 43 (2008) 268–273.

[43] M. Waheed, N. Ahmed, Tetrahedron Lett. 57 (2016) 3785–3789.

[44] J.G. Fierro-Arias, R. Redón, J.J. García, S. Hernández-Ortega, R.A. Toscano, D. Morales-Morales, J. Mol. Catal. 233 (2005) 17–27.

[45] E. Correa-Ayala, C. Campos-Alvarado, D. Chávez, S. Hernández-Ortega, D. Morales-Morales, V. Miranda-Soto, M. Parra-Hake, Inorg. Chim. Acta 490 (2019) 130–138.

[46] P. Pelagatti, A. Venturini, A. Leporati, M. Carcelli, M. Costa, A. Bacchi, G. Pelizzi, C. Pelizzi, Dalton Trans. (1998) 2715–2721.

[47] C. Herrera-Álvarez, V. Gómez-Benítez, R. Redón, J.J. García, S. Hernández-Ortega, R.A. Toscano, D. Morales-Morales, J. Organomet. Chem. 689 (2004) 2464–2472.

[48] R.H. Crabtree, The Organometallic Chemistry of Transition Metals, fourth ed., John Wiley & Sons, 2005.

[49] Y. Dang, S. Qu, J.W. Nelson, H.D. Pham, Z.-X. Wang, X. Wang, J. Am. Chem. Soc. 137 (2015) 2006–2014.

[50] J. Vicente, A. Arcas, F. Juliá-Hernández, D. Bautista, Angew. Chem. Int. Ed. 50 (2011) 6896–6899.

[51] F. Juliá-Hernández, A. Arcas, J. Vicente, Chem. Eur J. 18 (2012) 7780–7977.

[52] J.L. Bolliger, O. Blacque, C.M. Frech, Chem. Eur J. 14 (2008) 7969–7977.

[53] J. Liu, Y. Zhao, Y. Zhou, L. Li, T.Y. Zhang, H. Zhang, Org. Biomol. Chem. (2003) 3227–3231.

[54] H. Zhang, A. Lei, Dalton Trans. 40 (2011) 8745–8754.

[55] L. González-Sebastián, D. Morales-Morales, J. Organomet. Chem. 893 (2019) 39–51.